Appl. Phys. A 91, 365–368 (2008)
DOI: 10.1007/s00339-008-4448-8

Applied Physics A
Materials Science & Processing

A. ABDOLVAND[1,✉]
S.Z. KHAN[1,2]
Y. YUAN[2]
P.L. CROUSE[1]
M.J.J. SCHMIDT[1]
M. SHARP[3]
ZHU LIU[2]
LIN LI[1]

Generation of titanium-oxide nanoparticles in liquid using a high-power, high-brightness continuous-wave fiber laser

[1] Laser Processing Research Centre, School of Mechanical, Aerospace and Civil Engineering, The University of Manchester, Manchester M60 1QD, UK
[2] Corrosion and Protection Centre, School of Materials, The University of Manchester, Manchester M60 1QD, UK
[3] Lairside Laser Engineering Centre, University of Liverpool, Birkenhead CH41 9HP, UK

Received: 29 October 2007/Accepted: 15 February 2008
Published online: 4 March 2008 •

ABSTRACT Previous studies on laser-assisted nanomaterial formation in liquids have focused on using pulsed laser ablation of metals. We report, for the first time to our knowledge, the fabrication of nanoparticles via high-power high-brightness continuous-wave fiber laser ablation of titanium in liquids. Analysis revealed the generation of spherical nanoparticles of titanium-oxide ranging mainly between 5 nm and 60 nm in diameter. A mechanism of formation for crystallized nanoparticles, based on the self-organized pulsations of the evaporated metal, is proposed. This may account for the observed substantial efficiency gain owing to the high average power and brightness of the source.

PACS 42.62.-b; 81.07.-b; 52.50.-b; 47.20.-k; 45.55.-t

1 Introduction

Common techniques for the generation of nanoparticles using a laser beam include laser ablation, chemical vapor deposition or decomposition of gases, and physical vapour deposition [1]. The advantages of using lasers include narrower particles size distribution and less impurity. The above-mentioned techniques, however, generally require a vacuum chamber for the precise control of atmospheric conditions and temperature. Recently, laser ablation in liquid (LAL) for the generation of nanoparticles has been reported [2, 3], as an alternative technique for the controlled fabrication of various nanoparticles of noble metals [4], alloys [5, 6], oxides [7, 8] and semiconductors [9]. LAL facilitates the production of crystallized nanoparticles in a single step procedure without subsequent heat-treatment. In contrast to chemical methods of synthesis of nanoparticles, pure colloidal solutions can be formed without the formation of by-products. The entire product is collected in solution simplifying handling. Moreover, chemicals such as surfactants can be added to liquids in order to control the size and the aggregation state of nanoparticles due to the change of the surface charge of the nanoclusters [8]. Another advantage is that the production system is simple and does not require costly vacuum equipment.

So far, only pulsed laser sources, mainly nanosecond pulse lasers, have been employed in LAL [3, 10, 11]. There have been a number of attempts to explain the formation process of noble metals as well as metal-oxide nanoparticles by pulsed laser ablation in liquid (PLAL) [2–7, 10–13]. Generally speaking, for PLAL regime when very high irradiances (10^9–10^{10} W/cm^2) are applied, a laser-induced plasma is generated on the metallic target. The generated plasma is confined during each pulse, and expands at a supersonic velocity. This creates a shock front that in turn induces an elevated pressure and increase of plasma temperature [18, 19]. It is this transient pressure in front of the plasma plume that pushes the active species of metallic ions, atoms and clusters into the expanded plasma–liquid interfacial region. They then strongly react with molecules of the liquid forming nuclei of oxides and/or hydroxides. Thus, in the case of PLAL the plasma is confined and heated only during each pulse and the shock wave plays a self-limiting role for the generation of nanoparticles and alters the efficiency of the process. Furthermore, the process efficiency and the size of the colloidal particles are significantly influenced by the self-absorption of laser pulses by the colloidal particles, due to either "intra-pulse" or "inter-pulse" processes, i.e. the formation of colloidal particles in solution during any particular pulse, or between pulses [12]. It is mainly due to the fact that for pulsed ablation of a metal target a large number of laser pulses as well as long irradiation times (typically ranging from 15 min to 120 min) are required. It has to be mentioned that self-absorption by intra-pulse nanoparticles does not occur for femtosecond laser ablation, but the production efficiency under equivalent energy input is reported to be lower [13].

✉ Fax: +44-161-306-3803, E-mail: amin.abdolvand@manchester.ac.uk

We report, for the first time to our knowledge, on the high-rate generation of titanium-oxide nanoparticles in water and aqueous surfactant solutions using a high-power, high-brightness, continuous wave (cw) fiber laser source at 1070 nm. We show that the overall process time in this case is much shorter than PLAL, hence minimizing the self-absorption of irradiation by the colloidal particles. Titanium-oxide nanoparticles are very promising materials for a number of applications, such as gas sensors and photovoltaic cells [14, 15].

2 Experimental

The experimental setup for cw laser ablation in liquid (CWLAL) is fairly simple and similar to PLAL. Here, a high-purity titanium plate (99.999%), 1 mm in thickness, was first washed with ethanol and then with de-ionized water to remove organic contamination. It was then fixed at the bottom of a glass vessel filled with 8 ml of either de-ionized water or an aqueous solution of the surfactant sodium dodecyl sulfate (SDS) with a concentration of 0.01 M, which proved to be optimum for extended stability of the solution. It also encourages the formation of dispersed particles during laser ablation [3]. The thickness of the liquid layer above the target was kept to ~ 4 mm for the experiments. The output of the fiber laser [IPG single-mode YLR-1000-SM 1 kW fiber laser at $\lambda = 1070$ nm, and beam quality factor of 1.1 ($M^2 \sim 1.1$)], here 250 W, entered the solution from above at normal incident angle and was then focused on the target to a spot of $\sim D = 40\,\mu$m in diameter. The depth of focus (DOF $= \pm 0.08\pi D^2/M^2\lambda$) [17], i.e. the distance either side of the beam waist over which the beam diameter grows by 5%, is calculated to be $\sim 340\,\mu$m. The high brightness of the source facilitated the reasonably large DOF and hence negligible change of the spot size on the target. Thus, a uniform ablation trace was achieved throughout the experiments. High-brightness as well as the high output power of the source provides a high power density on the target. The maximum irradiance employed was 2×10^7 W/cm^2. Ablation time for the experiments reported here was 1 s corresponding to the total irradiation dose of 2×10^7 J/cm^2, which resulted in removal of approximately 0.4 mg of the target during each experiment. The process was monitored using a high-speed camera (PHANTOM V7, frame rate of $\sim 25\,000$ fps with a $\sim 37\,\mu$s exposure) using a Leitz monozoom microscope optical system.

The initial incident radiation on the surface of the target is estimated to be roughly 64% of the applied power (air–liquid interface 2%, liquid–target interface 30%, liquid absorption 4%). For the purpose of these experiments open cells were employed, therefore, on occasion, liquid droplets may have been ejected from the solution surface under laser irradiation. After completion of each experiment, the solutions were transferred to a vial and stored for subsequent analysis. No measurable loss of liquid volume during the course of our experiments was observed. Images of the particles were measured with transmission electron microscopy (TEM). TEM samples were prepared by placing a small drop of the obtained solutions onto a copper micro-grid and then allowing it to dry. Selected area electron diffraction (SAED) was used for crystallographic structure analysis of the products.

3 Results and discussion

Figures 1a and b show TEM images of particles in de-ionized water and solution of SDS, respectively. The images were recorded approximately 10 days after the experiments. The mean size and size distribution of particles, obtained by counting approximately 350 particles in the TEM images, are shown in the right side of each image. The size distribution of nanoparticles appears to be broadened in the SDS solution in comparison to the plain de-ionized water. Some large particles around 100 nm in diameter are observed in the SDS solution. However, smaller particles with diameters less than 10 nm are observed in SDS than in water. As would be expected the degree of agglomeration of nanoparticles is more pronounced for the particles prepared in de-ionized water (Fig. 1a). Shapes of the particles are spherical in both cases. The SAED pattern (inset in Fig. 1a), corresponds to the titanium-oxide nanoparticles in anatase phase, which was the predominant phase of nanoparticles in water. Both anatase and rutile phases are found for nanoparticles produced in SDS. The details of particles size, phase control and their characterisation will be presented elsewhere.

The mechanism of formation of nanoparticles for CWLAL is proposed as follows. At irradiances used in our experiments (of the order of 10^7 W/cm^2), a thin layer of the metal is heated above its evaporation temperature. Titanium possesses poor thermal conductivity (22 Wm^{-1}K^{-1} at 300 K) in comparison with other metals. It evaporates at 3287 °C at atmospheric pressure, corresponding to a specific enthalpy of 1.2×10^7 J/kg [20]. We estimate our surface enthalpy at 5×10^9 J/kg, two orders of magnitude above the evaporation threshold of titanium metal (the value is calculated by conservatively estimating the convective losses to the water to be 50%). We should like to point out that the evaporation threshold is the enthalpy required for complete evaporation of the meal. Thus, if the surface enthalpy is higher than the evaporation enthalpy, one could in principle conclude that the conditions are sufficient for some of the material to evaporate [17, 20]. This results in the intensive evaporation from the melt surface and formation of a plasma plume over the interaction spot (the generated vapor develops along the beam, and the large DOF maintained a high irradiance level owing to the high-brightness of the source). Owing to the violent evaporation of the solid target, the vapor contains highly energetic species of titanium atoms, ions and clusters. This is followed by the formation of a cavitation bubble in the liquid, as a result of the vaporization of a water layer in contact with the plasma. This was confirmed by monitoring the process using the high-speed camera. The bubble had a semi-spherical shape and was confined in the liquid. It is known that at high intensities evaporation is not stationary but has some characteristic pulsations, with the period close to the characteristic Rayleigh time for the bubbles collapse ($\sim 10^{-3}$ s) [21]. We believe that these pulsations push the highly energetic species into contact with the vaporized liquid inside the cavitation bubble.

Thus, nanoparticles appear to be formed due to the strong interaction between the high-energy species in the

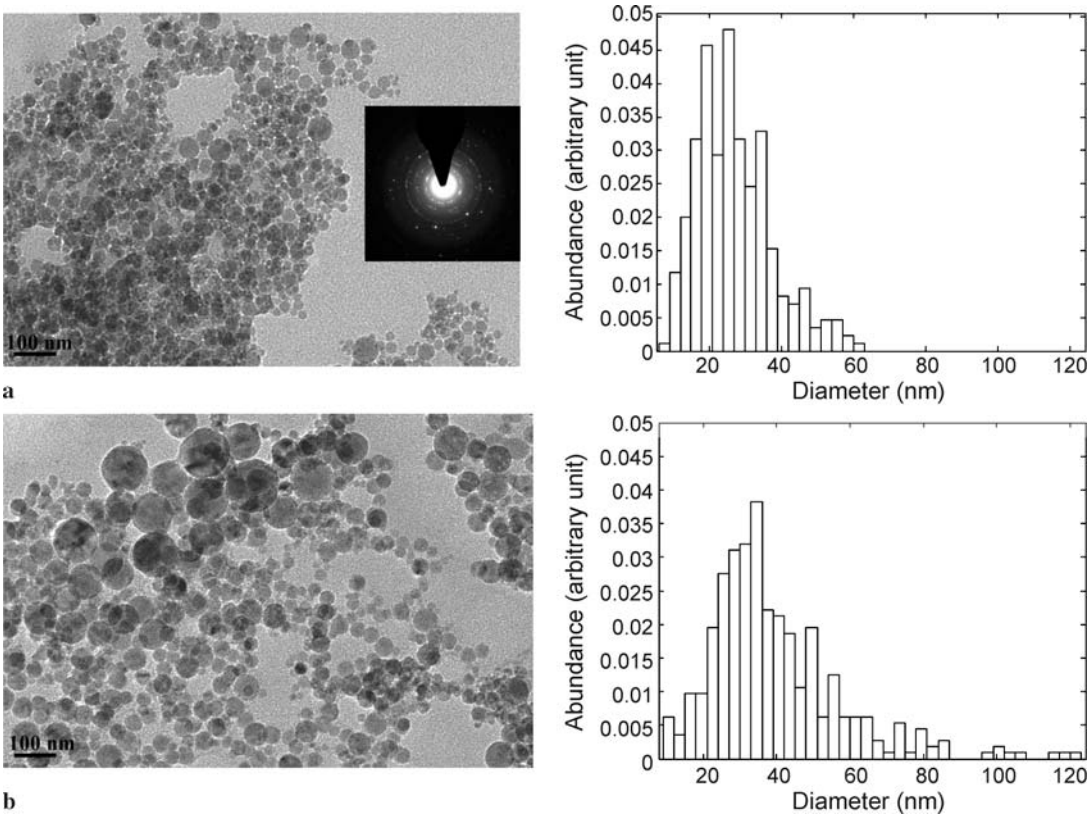

FIGURE 1 TEM images and size distribution of titanium-oxide nanoparticles prepared by CWLAL in (**a**) de-ionized water, and (**b**) SDS. The mean diameter d and the Gaussian standard deviation σ of the nanoparticles: (**a**) $d = 27$ nm, $\sigma = 11$ nm; (**b**) $d = 40$ nm, $\sigma = 18$ nm. *Inset* to (**a**): Diffraction pattern from nanoparticles (SAED pattern)

steep temperature gradient at the edges of the plasma plume, where cooler temperatures allow the existence of the titanium oxides species. The growth process is quenched upon collapse of the bubble and contact between the particles and the liquid. It is worth noting that the collapse of the cavitation bubble increases the temperature and pressure of the gas within [22]. This results in the violent dissipation of the vapor into the surrounding liquid with the consequence of releasing a significant amount of energy as visible light and/or an acoustic shock wave.

Our initial calculations of the system composition at chemical thermodynamic equilibrium indicates that titanium metal and its vapor react with water to form oxides and some hydroxides depending on conditions, with the evolution of hydrogen gas. In fact a wide range of oxide phases, ranging from rutile and anatase, through the mixed stoichiometries to the monoxide were produced. So far, thus, analyses of the product support these calculations. Evaporation thus would result in the aggregation of metal oxide and hydroxide molecules, which themselves will then serve as growth nuclei. The quench rate induced by the de-ionized water appears to be more rapid than with SDS, resulting in the marginally narrower size distribution and smaller average particle diameter. This result was somewhat unexpected and will require further investigation. The presence of the surfactant, however, improved the stability of the suspension after its formation and prevented agglomeration of the particles.

We should like to highlight that even a very short exposure time of 1 s was enough to remove ~ 0.4 mg of the material, resulting in the consumption energy of 625 kJ/g (specific energy of approximately 174 kWh/kg). This implies a scaled production rate of ~ 1–1.5 g/h, close to the established wet chemical approaches such as sol–gel and precipitation techniques. To the best of our knowledge, only Nichols et al. [23] has recently reported a production rate of 4.4 mg/h (specific energy of approximately 3086 kWh/kg) for pulsed laser ablation of platinum metal target in water using a pulsed Nd:YAG laser. It is worth noting that the comparison between the two methods is in relation to the expended energy and time effort required, with potential view to an industrial production process.

4 Conclusions

In order to continually produce dispersions of nanoparticles at high rates, processes with continuous supply and drain of the liquid can be applied. Further aspects including scope for scale-up for production of customized nanoparticles using high-power high-brightness cw laser sources, require further investigation. However, our preliminary results/estimations show that the size, size distribution and phases of nanoparticles can depend on the laser parameters and the type of environment. These aspects form the subject matter of a more detailed paper now in preparation.

ACKNOWLEDGEMENTS This work was conducted by the Northwest Laser Engineering Consortium, funded by the Northwest Development Agency (NWDA) of the United Kingdom. The high-speed imaging system and monozoom microscope were on loan from the EPSRC Engineering Instrument Pool. The authors

are very grateful to Prof. B.S. Luk'yanchuk for fruitful discussions.

REFERENCES

1 P. Heszler, L. Landstrom, Proc. SPIE **5118**, 60 (2003)
2 J. Neddersen, G. Chumanov, T.M. Cotton, Appl. Spectrosc. **47**, 1959 (1993)
3 F. Mafune, J. Kohno, Y. Takeda, T. Kondow, J. Phys. Chem. B **107**, 4218 (2003)
4 T. Tsuji, N. Watanabe, M. Tsuji, Appl. Surf. Sci. **211**, 189 (2003)
5 S.H. Tsai, Y.H. Liu, P.L. Wu, C.S. Yeh, J. Mater. Chem. **13**, 978 (2003)
6 J. Zhang, J. Worley, S. Denommee, C. Kingston, Z.J. Jakubek, Y. Deslandes, M. Post, B. Simard, N. Braidy, G.A. Botton, J. Phys. Chem. B **107**, 6920 (2003)
7 A. Iwabuchi, C.K. Choo, K. Tanaka, J. Phys. Chem. B **108**, 10 863 (2004)
8 H. Usui, T. Sasaki, N. Koshizaki, Appl. Phys. Lett. **87**, 0 631 051 (2005)
9 K.V. Anikin, N.N. Melnik, A.V. Smakin, G.A. Shafeev, V.V. Voronov, A.G. Vitukhnovsky, Chem. Phys. Lett. **366**, 357 (2002)
10 A.V. Simakin, V. Voronov, N. Kirichenko, G. Shafeev, Appl. Phys. A **79**, 1127 (2004)
11 J.S. Golightly, A.W. Castleman Jr., J. Phys. Chem. B **110**, 19 979 (2006)
12 T. Tsuji, K. Iryo, Y. Nishimura, M. Tsuji, J. Photochem. Photobiol. A **145**, 201 (2001)
13 T. Tsuji, T. Kakita, M. Tsuji, Appl. Surf. Sci. **206**, 314 (2003)
14 G. Williams, G.S.V. Coles, J. Mater. Chem. **8**, 1657 (1998)
15 P.V. Kamat, *Nanoparticles and Nanostructures Films*, ed. by J.H. Fendler (Wiley-VCH, Weinheim, 1998)
16 J.P. Sylvestre, A.V. Kabashin, E. Sacher, M. Meunier, J.H.T. Luong, J. Am. Chem. Soc. **126**, 7176 (2004)
17 W.M. Steen, *Laser Material Processing* (Springer, Heidelberg, 2003)
18 R. Fabbro, J. Fournier, P. Ballard, D. Devaux, J. Virmont, J. Appl. Phys. **68**, 775 (1990)
19 L. Berthe, R. Fabbro, P. Peyre, L. Tollier, E. Bartnicki, J. Appl. Phys. **82**, 2826 (1997)
20 M. von Allmen, A. Blatter, *Laser-beam Interactions with Materials* (Springer, Berlin, 1995)
21 A.A. Vedenov, G.G. Gladush, *Physical Processes in Laser Processing of Materials* (Energoatomizdat, Moscow, 1985) [in Russian]
22 C.E. Brennen, *Cavitation and Bubble Dynamics* (Oxford University Press, Oxford, 1995)
23 W.T. Nichols, T. Sasaki, N. Koshizaki, J. Appl. Phys. **100**, 114 912 (2006)